

# Luttinger Liquid in the Core of Screw Dislocation in Helium-4

M. Boninsegni,<sup>1</sup> A.B. Kuklov,<sup>2</sup> L. Pollet,<sup>3</sup> N.V. Prokof'ev,<sup>4,5</sup> B.V. Svistunov,<sup>4,5</sup> and M. Troyer<sup>3</sup>

<sup>1</sup>*Department of Physics, University of Alberta, Edmonton, Alberta T6G 2J1*

<sup>2</sup>*Department of Engineering Science and Physics, CUNY, Staten Island, NY 10314*

<sup>3</sup>*Theoretische Physik, ETH Zürich, CH-8093 Zürich, Switzerland*

<sup>4</sup>*Department of Physics, University of Massachusetts, Amherst, MA 01003, USA*

<sup>5</sup>*Russian Research Center "Kurchatov Institute", 123182 Moscow, Russia*

(Dated: November 16, 2018)

On the basis of first-principle Monte Carlo simulations we find that the screw dislocation along the hexagonal axis of an *hcp* <sup>4</sup>He crystal features a superfluid (at  $T \rightarrow 0$ ) core. This is the first example of a regular quasi-one-dimensional supersolid – the phase featuring both translational and superfluid orders, and one of the cleanest cases of a Luttinger-liquid system. In contrast, the same type of screw dislocation in solid H<sub>2</sub> is insulating.

PACS numbers: 75.10.Jm, 05.30.Jp, 67.40.Kh, 74.25.Dw

The remarkable observations of a non-classical moment of inertia in solid <sup>4</sup>He [1, 2, 3, 4, 5] have sparked a wave of interest in the supersolid state of matter (see review [6] and references therein). According to the standard paradigm [7], the uniform supersolid state develops if the energy gap for creating vacancies vanishes in the ground state of a crystal, leading to a finite concentration of stable and delocalized vacancies. In the past, however, experiments did not find such zero-point vacancies [8]. Recent Monte Carlo simulations of solid <sup>4</sup>He [9, 10, 11, 12] have further limited possible mechanisms for a uniform supersolid state: A perfect *hcp* <sup>4</sup>He crystal is an insulator with a large energy gap toward vacancy creation and an even larger one for interstitials. When vacancies are introduced by hand into a perfect *hcp* crystal, they undergo phase separation [9]. This provides strong evidence that a <sup>4</sup>He crystal does not conform to any standard supersolid scenario.

The situation is quite different for defect-ridden, or polycrystalline *hcp* <sup>4</sup>He. Simulations showed that grain boundaries are generically superfluid [13], while a recent experiment observed superflow in non-uniform samples and attributed it to the presence of grain boundaries [14]. In general, two types of supersolid may exist – regular and glassy. While in both cases translational symmetry is broken, regular supersolid is characterized by two orders – discrete translational and superfluid. Thus, due to lack of discrete translational order, the superfluid grain boundaries do not constitute an example of a regular supersolid. They should rather be considered as superglass.

One may conjecture that (straight) dislocations, featuring translational order, might host SF along their cores [15, 16]. More recently, a phenomenological model was proposed, where crystal deformations [17], particularly inside a dislocation core [18], promote SF see also Ref. [19] on role of <sup>3</sup>He in inducing superfluidity in dislocation cores. None of the previous theories, however, was quantitative and conclusive. The model [17, 18] contrasts with our observation of insulating grain boundaries with small tilt angles because this type of boundary can be considered as a wall of rarely spaced *edge* dislocations

[13, 20]. We are not aware of any suggestion that screw dislocations have any advantage over edge dislocations in terms of their SF properties; on the contrary, they were often excluded from the list. Thus, the question remains: Do extended supersolid defects characterised by translational and superfluid orders exist in <sup>4</sup>He crystals? In this Letter, we give an affirmative answer to this question, i.e., we provide theoretical evidence of SF inside the core of a screw dislocation aligned with the *c*-symmetry axis of *hcp* <sup>4</sup>He.

Our grand-canonical Monte Carlo simulations are based on the worm algorithm, i.e., a Path Integral Monte Carlo technique defined on the configuration space for the single-particle Matsubara Green function [21]. For spatial imaging, we employ the winding-cycle maps, i.e., averaged set of points measuring instant spatial position of a randomly selected element (bead) of the worldline with non-zero winding number (winding cycle). The winding cycles define the superfluid response [22], so that the winding-cycle map allows one to visualize the spatial distribution of the superfluid component. Qualitatively speaking, a winding-cycle map represents the local superfluid response.

*Sample geometry.* The geometry of our sample is illustrated in Figs. 1 and 2. The sample is periodic in the *z*-direction, with 8 pairs of basal planes. In order to rule out finite-size effects, we have simulated samples with 3 and 4 pairs of basal planes as well.

Cell periodicity in the *xy* plane is incompatible with the presence of a single dislocation. One could restore it by simulating a dislocation pair, but we opt instead for a single dislocation, using a non-periodic cell in the *xy* plane, as this allows us to *a*) simulate samples with the rotational symmetry of a *hcp* crystal *b*) obtain robust results with smaller samples.

Our simulation sample consists of an ideal *hcp* crystal with a screw dislocation in its center along the *c* axis. Specifically, we, first, superimpose two identical triangular layers separated by half of the *c*-axis period  $a_z = \sqrt{8/3}a$  along the *c*-axis and shifted by  $(a/2, a/\sqrt{3})$  in the *xy*-plane, *a* being the lattice period along the *x*-

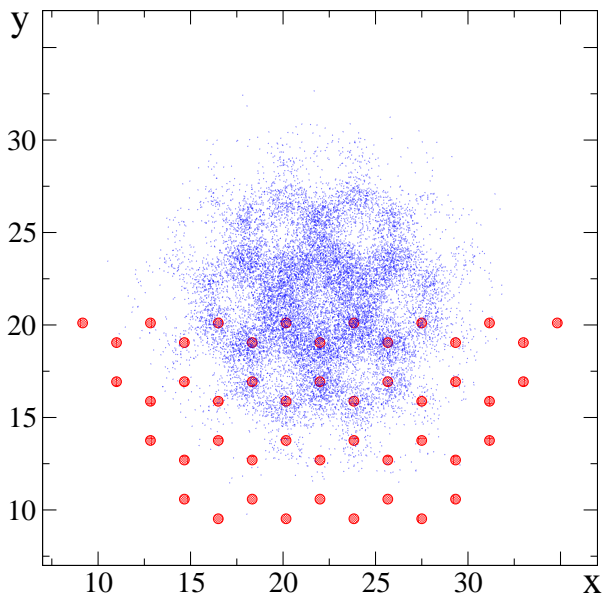


FIG. 1: (Color online. For the best perception, look from a distance.) Columnar winding-cycle map (blue dots) in the core of the screw dislocation in solid  ${}^4\text{He}$  at  $T = 0.25$  K and density  $0.0287 \text{ \AA}^{-3}$ . View is along the hexagonal axis, with the core parallel to it. Shown with red dots (in the lower half of the plot only) are the atomic positions in the initial configuration. At distances  $\sim 3a$  from the core, the atomic positions averaged over the imaginary time are only slightly shifted against those of the original configuration. The unit of length is  $1 \text{ \AA}$ .

axis. The crystal, then, has been cut along the  $xz$ -half-plane, whose edge (located at the center of one of the hexagons formed when all basal layers are projected to a single  $xy$ -plane) is the dislocation core. Atoms have been displaced so that, upon completing a full revolution around the core, each atom advances by a lattice period  $a_z$ . This procedure creates an ideal (classical) screw dislocation in essentially infinite medium. Then, all particles located outside a (pencil shape) cylinder, with the dislocation core being its axis of symmetry, (and inside the rectangular simulation cell) have been pinned. These particles are not moved in our Monte Carlo simulation, but they do interact with the rest of the system via the helium pair potential. The purpose of these “frozen” particles is that of confining our sample to the inner (cylindrical) part of the cell, while, practically, completely eliminating the effects of open boundary conditions. Our rectangular simulation cell is twice the size of the physical sample inside the cylinder. The initial numbers of (physical) atoms used in simulations are  $N_{ini} = 384, 768, 1912$ .

*Superfluid response.* The simulations were performed at the number density  $0.0287 \text{ \AA}^{-3}$ , that is, in the close vicinity of the melting point. The lattice period along

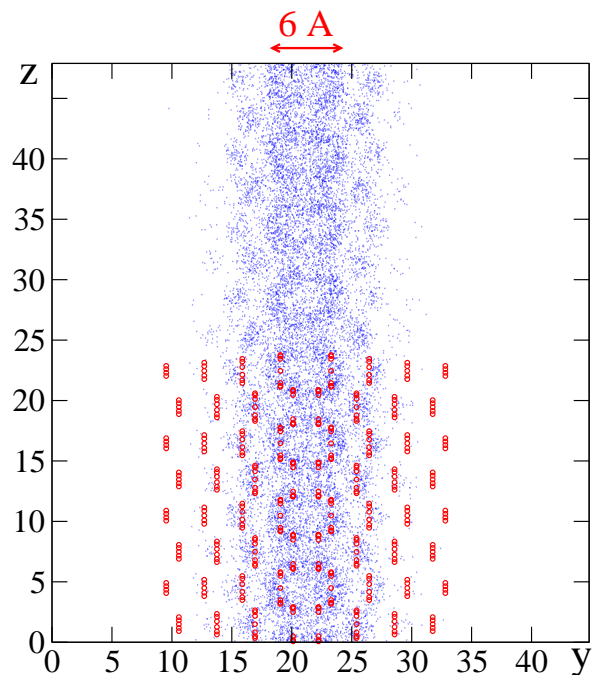


FIG. 2: (Color online.) Columnar winding-circle map in the core of screw dislocation. View is along the  $x$ -axis in the basal plane—perpendicular to the core. Shown with red dots (in the lower half of the plot only) are the atomic positions in initial configuration. The unit of length is  $1 \text{ \AA}$ .

the  $x$ -direction is then  $a = 3.666 \text{ \AA}$ . The convenience of working at the melting point is that we know the chemical potential,  $\mu = 0.02 \text{ K}$ , from the simulations of the liquid phase at its freezing density [21]. Our simulations span a temperature range from  $0.2$  to  $1 \text{ K}$ .

In Figs. 1 and 2 we present the projected winding-cycle maps on the  $xy$ - and  $yz$ -planes, together with the initial configuration of the atoms. We see that the superfluid density in the dislocation core is strongly correlated with the insulating environment, respecting the hexagonal symmetry modified by the presence of the screw dislocation. The superfluid density is most robust along the bonds of the ideal structure.

Quantitatively, our data can be analyzed using the concepts of Luttinger liquid theory. Luttinger liquids are characterized by two parameters, the superfluid stiffness  $\Lambda_s = n_s^{(1D)}/m$  (where  $n_s^{(1D)}$  is the 1D superfluid density and  $m$  is the helium atom mass) and the compressibility  $\kappa$ . Both can be extracted from the distributions  $P_W(W)$ ,  $P_N(N)$  of the winding  $W$  (along the core) and particle number  $N$  fluctuations directly obtained in the simulation:

$$\begin{aligned} P_W(W) &\sim \exp\left(-\frac{LW^2}{2\beta\Lambda_s}\right), \\ P_N(N) &\sim \exp\left(-\frac{\beta N^2}{2L\kappa}\right), \end{aligned} \quad (1)$$

where  $N$  is taken relative to its mean  $\langle N \rangle$  [23],  $L$  is the sample length along the  $c$ -axis and  $\beta$  stands for inverse temperature. We fitted the collected histograms  $P_W(W)$ ,  $P_N(N)$  with Gaussians and have obtained the superfluid stiffness and the compressibility. The Luttinger parameter is given as  $K_L^{-1} = \pi\sqrt{\Lambda\kappa}$ . Our data (for the different temperatures, and different system sizes in the  $z$ -direction) yield  $K_L = 0.205(20)$ , where the finite-size (along the  $c$ -axis) and statistical errors are combined. The initial number of (updatable) particles in the state shown in Figs. 1 and 2 was  $N = 768$  corresponding to a relatively tight confinement in the  $xy$ -plane. We clearly see superfluidity in samples with much larger number of particles in the  $xy$ -plane (1912 updatable particles in the sample with 3 pairs of basal planes). In particular, the superfluid stiffness was found to be the same within the error bars (of about 20%). However, the accuracy of data for  $\kappa$  was not sufficient for resolving finite-size effects in  $K_L$  due to the  $xy$ -confinement.

For the value of the chemical potential corresponding to the melting point, the average equilibrium number of particles in the 8 basal-pair sample was found to be about 770. By varying chemical potential and, in particular, lowering it below the point where  $N = 768$ , we saw no qualitative difference in the superfluid response, which is fully consistent with the fact that  $K_L < 1/2$  (in the Luttinger liquid, an external periodic potential is relevant for opening the insulating gap only at  $K_L > 1/2$  [24, 25, 26, 27]). A sample half the size in  $z$ -direction yielded the same qualitative conclusion. In the 3 basal-pair sample with much larger number of particles in the  $xy$ -plane, we observe that the core dopes itself with vacancies (of the order of 3-4), rather than with interstitial atoms, apparently due to lower effective chemical potential in the core. We do not attribute special significance to this fact because by increasing the chemical potential by 4 K, far smaller than the interstitial energy in the *hcp* solid, the system can be made to have the original (classical solid) particle number without changing the superfluid nature of the state.

From our data for  $\Lambda_s$  we deduce that  $n_s^{(1D)}$  is about 1 particle per 1 Å, which is equivalent to saying that superfluid phase in the dislocation core involves nearly all atoms in a “tube” of diameter 6 Å. More quantitatively, one can assign the superfluid response to partial contributions from the coordination shells. Nearly 90 % of points in the winding-cycle map in Fig. 1 belong to the first three coordination shells with the following division: 35 % in the first shell, 29 % in the second one, and 26 % in the third one.

Special care should be taken to make sure that the observed superfluid response is not an artifact of poor thermalization of the worldline configurations in the dislocation core. This concern stems from our previous experience with edge dislocations, where we saw that a superfluid glassy region in the core—created either by hand, or as a result of quenched relaxation of the initial configuration—remains essentially metastable, at least at

temperatures  $\sim 0.2$  K. To rule out such a scenario, we first relaxed the initial configuration by treating atoms as classical particles with a repulsive potential  $\sim 1/r^6$ , and minimizing the energy of the configuration. [In the case of edge dislocations, this protocol leads to an insulating groundstate.] Our observation was that in both cases—with or without classical relaxation—the Monte Carlo process converges to one and the same result. Another indication that our superfluid signal is not an artifact of poor thermalization comes from the perfect regularity of the superfluid density map, in combination with its strong correlation to the insulating environment. This outcome rules out concerns based on a lack of thermalization in the glassy state. Analogous simulations have been performed for the *hcp para*-hydrogen crystal, using the same sample preparation procedure, at a density of  $0.0261 \text{ \AA}^{-3}$ , corresponding to the  $T \rightarrow 0$  equilibrium density. In this case, the dislocation core is found to be an insulator *doped with vacancies* (forming a commensurate density wave).

*Discussion.* The observation of a superfluid dislocation in a  $^4\text{He}$  crystal is an interesting example of a regular quasi-one-dimensional supersolid. However, the question is whether this observation is relevant to the effect of non-classical inertia [1]. Superfluid dislocations can be a part of the disordered superfluid network, together with superfluid grain boundaries, ridges, and liquid (or glassy, at higher pressure) pockets, etc. Considering a network of dislocations only, the effective three-dimensional superfluid fraction of such a network is limited by the volume fraction of the atoms located at the cores of dislocations. This fraction is likely to be significantly smaller than  $\sim 1\%$ . The dislocation density in solid  $^4\text{He}$  typically varies over a range as wide as  $10^6 \div 10^{10} \text{ cm}^{-2}$  [28, 29, 30, 31, 32]. It is, however, also possible to grow crystal without screw dislocations at all [33]. Taking the 1D superfluid density of  $n_s^{(1D)} \approx 1 \text{ \AA}^{-1}$  observed in our simulations, we estimate the required order-of-magnitude dislocation density  $n_d \sim 1/l^2 \sim 3 \times 10^{12} \text{ cm}^{-2}$  in order to account for  $n_s^{(3D)}/n = (n_s^{(1D)}n_d)/n \sim 1\%$  of the superfluid fraction observed in [1]. Here  $l$  is the typical distance between dislocations.

The Luttinger liquid parameter is all we need to characterize superfluid properties of the dislocation network consisting of segments of length  $l \gg a$ . As it has been pointed out by Shevchenko [34], in this system one has to distinguish between static and dynamic responses. Below the thermodynamic transition temperature  $T_c \sim T_*a/l$  (which can be also written as  $T_c \sim T_*[n_s^{(3D)}/n]^{1/2}$ , in terms of the zero-point superfluid fraction  $n_s^{(3D)}/n$ ) the network features a non-zero static superfluid response [34]. Here,  $T_*$  is the characteristic temperature of the superfluid helium liquid. In our simulations we find that the core has robust phase coherence properties at all temperatures below 1 K, which allows us to set  $T_* \sim 1$  K (the continuation of the  $\lambda$ -line in liquid helium to the region of solid densities gives  $T_\lambda \approx 1.5$  K [13]). This estimate is

in agreement with the small value of  $K_L$ .

In the temperature range  $T_c < T < T_*$ , which is very broad for large aspect ratio  $l/a$ , the state of the system can be viewed as a vortex tangle with ‘vortex cores’ (which are not well defined geometric objects because of the natural uncertainty  $\sim l$  in their sizes and positions) pinned in the solid bulk. We refer to this state as Shevchenko state [34]. In contrast to the original purely classical analysis of Ref. [34], we emphasize that the dynamics of Shevchenko state should be driven by discrete *quantum-tunneling* phase slip events (instantons), with the typical relaxation time  $\tau \sim (T_*/T)^{8/K_L-1}/T_*$ , as it follows from the microscopic analysis [35]. In the low-frequency limit  $\omega\tau \ll 1$  the state is essentially normal. At ‘high’ frequencies  $\omega\tau \gg 1$  the response is nearly indistinguishable from the standard superfluid [34]. Note also, that for  $K_L \ll 1$  and  $T \ll T_*$  the phase-slip time can easily exceed any realistic experimental time-scale making it very hard to detect the genuine thermodynamic transition at  $T_c$ .

While being focused on one isolated screw dislocation, we note that small twist-angle grain boundary can be represented as an array of screw dislocations [20] and, there-

fore, must also be superfluid with an additional feature of tunneling coupling between the cores. Such boundaries might be the most realistic objects for studies of superfluidity of screw dislocations.

In summary, we have found that the screw dislocation in *hcp* solid  $^4\text{He}$  supports (at  $T \rightarrow 0$ ) superfluid transport of  $^4\text{He}$  atoms along its core, yielding thus the first realistic example of a regular continuous supersolid. Analogous dislocation in the *hcp* solid  $\text{H}_2$  is found to be an insulator.

The authors acknowledge valuable discussions with Alex Meyerovich, Moses Chan, Miko Palaanen, Sergei Shevchenko and Sebastien Balibar. This work was supported by the Swiss National Fund, the National Science Foundation under Grants Nos. PHY-0426881, PHY-0426814 and PHY-0456261, and by the Natural Science and Engineering Research Council of Canada under grant G12120893. We recognize an essential role of (super)computer clusters at UMass, Typhon at CSI, Hreidar at ETH, and AICT, University of Alberta. N. P. and B. S. acknowledge partial support from CRDF under Grant 2853. A.K. acknowledges partial support from PSC-CUNY Grant 68230-0037.

- 
- [1] E. Kim and M.H.W. Chan, *Nature*, **427**, 225 (2004); *Science* **305**, 1941 (2004).
- [2] A.S.C. Rittner and J.D. Reppy, *Phys. Rev. Lett.* **97**, 165301 (2006).
- [3] M. Kondo, S. Takada, Y. Shibayama, and K. Shirahama, *cond-mat/0607032* (to appear in *J. of Low Temp. Phys.*)
- [4] A. Penzev, Y. Yasuta, and M. Kubota, *cond-mat/0702632* (to appear in *J. of Low Temp. Phys.*)
- [5] A.S.C. Rittner and J.D. Reppy, *Phys. Rev. Lett.* **98**, 175302 (2007).
- [6] N.V. Prokof'ev, *Advances in Physics*, **56**, 381 (2007).
- [7] A.F. Andreev and I.M. Lifshitz, *Sov. Phys. JETP* **29**, 1107 (1969); G.V. Chester, *Phys. Rev. A* **2**, 256 (1970).
- [8] B.A. Fraass, P.R. Granfors and R.O. Simmons, *Phys. Rev. B* **39**, 124 (1989); M.W. Meisel, *Physica B* **178**, 121 (1992).
- [9] M. Boninsegni, A.B. Kuklov, L. Pollet, N.V. Prokof'ev, B.V. Svistunov, and M. Troyer, *Phys. Rev. Lett.* **97**, 080401 (2006).
- [10] D.M. Ceperley and B. Bernu, *Phys. Rev. Lett.* **93**, 155303 (2004).
- [11] M. Boninsegni, N. Prokof'ev, and B. Svistunov, *Phys. Rev. Lett.* **96**, 105301 (2006).
- [12] B.K. Clark and D.M. Ceperley, *Phys. Rev. Lett.* **96**, 105302 (2006).
- [13] L. Pollet, M. Boninsegni, A.B. Kuklov, N.V. Prokof'ev, B.V. Svistunov, and M. Troyer, *Phys. Rev. Lett.* **98**, 135301 (2007).
- [14] S. Sasaki, R. Ishiguro, F. Caupin, H.J. Maris, and S. Balibar, *Science* **313**, 1098 (2006).
- [15] S.I. Shevchenko, *Sov. J. Low Temp. Phys.* **13**, 61 (1987).
- [16] A. Meyerovich, private communication.
- [17] A.T. Dorsey, P.M. Goldbart, and J. Toner, *Phys. Rev. Lett.* **96**, 055301 (2006).
- [18] J. Toner, unpublished (as reported by A. T. Dorsey, APS March Meeting 2007, talk V1.000010).
- [19] E. Manousakis, *EPL* **78**, 36002(2007).
- [20] J. M. Burgers, *Proc. Phys. Soc.* **52**, 23 (1940); W. L. Bragg, *Proc. Phys. Soc.* **52**, 105 (1940).
- [21] M. Boninsegni, N. Prokof'ev, and B. Svistunov, *Phys. Rev. Lett.* **96**, 070601 (2006); *Phys. Rev. E* **74**, 036701 (2006).
- [22] E.L. Pollock and D.M. Ceperley, *Phys. Rev. B* **36**, 8343 (1987).
- [23] N.V. Prokof'ev, B.V. Svistunov, and I.S. Tupitsyn, *JETP* **87**, 310 (1998).
- [24] S. Coleman, *Phys. Rev. D*, **11**, 2088 (1975).
- [25] S.T. Chui and P.A. Lee, *Phys. Rev. Lett.* **35**, 315 (1975).
- [26] F.D.M. Haldane, *Phys. Rev. Lett.* **47**, 1840 (1981).
- [27] T. Giamarchi and H.J. Schulz, *Phys. Rev. B* **37**, 325 (1988).
- [28] V.L. Tsymbalenko, *Sov. Phys. JETP* **49**, 859 (1979).
- [29] I. Iwasa, K. Araki, and H. Suzuki, *J. Phys. Soc. Jpn.* **46**, 1119 (1979).
- [30] A.A. Golub and S.V. Svatko, *Sov. J. Low Temp. Phys.* **6**, 465 (1980).
- [31] Y. Hiki and F. Tsuruoka, *Phys. Rev. B* **27**, 696 (1983).
- [32] Yu. A. Kosevich and S.V. Svatko, *Sov. J. Low Temp. Phys.* **9**, 99 (1983).
- [33] J. P. Ruutu, P. J. Hakonen, A. V. Babkin, A. Ya. Parshin, J. S. Penttilä, J. P. Saramäki, and G. Tvalashvili, *Phys. Rev. Lett.* **76**, 4187 (1996).
- [34] S.I. Shevchenko, *Sov. J. Low Temp. Phys.* **14**, 553 (1988).
- [35] V.A. Kashurnikov, A.I. Podlivaev, N.V. Prokof'ev, and B.V. Svistunov, *Phys. Rev. B*, **53**, 13091 (1996); Yu. Kagan, N.V. Prokof'ev, and B.V. Svistunov, *Phys. Rev. A*, **61**, 045601 (2000).